

# Analysis of Mammalian Carboxylesterase Inhibition by Trifluoromethylketone-Containing Compounds

Randy M. Wadkins, Janice L. Hyatt, Carol C. Edwards, Lyudmila Tsurkan, Matthew R. Redinbo, Craig E. Wheelock,<sup>1</sup> Paul D. Jones, Bruce D. Hammock, and Philip M. Potter

*Department of Chemistry and Biochemistry, University of Mississippi, University, Mississippi (R.M.W.); Department of Molecular Pharmacology, St. Jude Children's Research Hospital, Memphis, Tennessee (J.L.H., C.C.E., L.T., P.M.P.); Department of Chemistry, University of North Carolina at Chapel Hill, Chapel Hill, North Carolina (M.R.R.); Department of Entomology and Cancer Research Center, University of California Davis, Davis, California (C.E.W., P.D.J., B.D.H.).*

Received December 13, 2005; accepted December 12, 2006

## ABSTRACT

Carboxylesterases (CE) are ubiquitous enzymes that hydrolyze numerous ester-containing xenobiotics, including complex molecules, such as the anticancer drugs irinotecan (CPT-11) and capecitabine and the pyrethroid insecticides. Because of the role of CEs in the metabolism of many exogenous and endogenous ester-containing compounds, a number of studies have examined the inhibition of this class of enzymes. Trifluoromethylketone-containing (TFK) compounds have been identified as potent CE inhibitors. In this article, we present inhibition constants for 21 compounds, including a series of sulfanyl, sulfinyl, and sulfonyl TFKs with three mammalian CEs, as well as human acetyl- and butyrylcholinesterase. To examine the nature of the slow tight-binding inhibitor/enzyme interaction, assays were performed using either a 5-min or a 24-h preincubation period. Results showed that the length of the preincu-

bation interval significantly affects the inhibition constants on a structurally dependent basis. The TFK-containing compounds were generally potent inhibitors of mammalian CEs, with  $K_i$  values as low as 0.3 nM observed. In most cases, thioether-containing compounds were more potent inhibitors than their sulfinyl or sulfonyl analogs. QSAR analyses demonstrated excellent observed versus predicted values correlations ( $r^2$  ranging from 0.908–0.948), with cross-correlation coefficients ( $q^2$ ) of  $\sim 0.9$ . In addition, pseudoreceptor models for the TFK analogs were very similar to structures and models previously obtained using benzil- or sulfonamide-based CE inhibitors. These studies indicate that more potent, selective CE inhibitors, containing long alkyl or aromatic groups attached to the thioether chemotype in TFKs, can be developed for use in vivo enzyme inhibition.

Carboxylesterases (CE) have been identified in organisms ranging from bacteria to humans and are thought to be responsible for the detoxification of xenobiotics (Cashman et al., 1996). CEs (EC 3.1.1.1) are members of the  $\alpha/\beta$  hydrolase

family and cleave carboxylesters (RCOOR') into the corresponding carboxylic acid (RCOOH) and alcohol (R'OH) via a proton transfer hydrolysis mechanism using a catalytic serine present within a Ser-His-Glu triad (Redinbo and Potter, 2005). These enzymes metabolize numerous clinically useful drugs (e.g., CPT-11, capecitabine, meperidine) as well as the illicit compounds heroin and cocaine, and commercial pesticides (e.g., permethrin, malathion) (Ahmad and Forghash, 1976; Potter et al., 1998; Wheelock et al., 2005; Ross et al., 2006). Consequently, the development of specific CE inhibitors may have both therapeutic and commercial utility (Hammock et al., 1982; Ashour and Hammock, 1987; Linderman et al., 1989).

Some of the most potent CE inhibitors identified to date are a group of compounds collectively known as trifluoromethyl ketones (TFKs; RCOCF<sub>3</sub>). These compounds contain

This work was supported in part by National Institutes of Health (NIH) grants CA76202, CA79763, CA98468, CA108775, Cancer Center Core grant P30-CA21765, National Institute of Environmental Health Sciences (NIEHS) grant R37-ES02710, NIEHS Superfund grant P42-ES04699, NIEHS Center for Environmental Health Sciences grant P30-ES05707, and by the American Lebanese Syrian Associated Charities. C.E.W. was supported by a Japanese Society for the Promotion of Science (JSPS) postdoctoral fellowship and NIH postdoctoral training grant T32-DK07355-22. P.D.J. was supported by NIH/National Heart, Lung, and Blood Institute Ruth L. Kirschstein National Research Service Award grant F32-HL078096.

<sup>1</sup> Current affiliation: Microbiology and Tumor Biology Center, Karolinska Institute, Stockholm, Sweden.

Article, publication date, and citation information can be found at <http://molpharm.aspetjournals.org>. doi:10.1124/mol.105.021683.

**ABBREVIATIONS:** CE, carboxylesterase; CPT-11, irinotecan; TFK, trifluoromethyl ketone; AChE, acetylcholinesterase; QSAR, quantitative structure-activity relationship; 3D, three-dimensional; BChE, butylcholinesterase; h, human; r, rabbit; Mp, melting point; o-NPA, o-nitrophenyl acetate.

a trifluoromethyl group in the  $\alpha$  position with respect to the ketone moiety (Fig. 1). The trifluoroacyl chemotype is very efficient at inhibiting enzymes whose catalytic mechanism involves attack by a nucleophilic catalytic residue (e.g., serine). The resulting tetrahedral TFK adduct contains the trifluoromethyl group, the protein (via the serine residue), a C-O<sup>-</sup> oxyanion (from the ketone oxygen), and the respective inhibitor moiety (e.g., an alkyl chain). However, as the trifluoromethyl group is a poor leaving group, the enzyme is reversibly inhibited. The extreme potency of these compounds is attributed to the polarization of the carbonyl by the trifluoromethyl group, which greatly increases the electrophilicity of the carbonyl carbon and hence its susceptibility to nucleophilic attack (Székács et al., 1992). Of particular interest is the observation that in TFK-containing inhibitors or in more broadly polarized ketones, the polarization of the carbonyl group shifts the equilibrium toward the *gem*-diol form (Fig. 1) (Roe et al., 1997).

TFKs were first studied as inhibitors of acetylcholinesterase (AChE) (Brodbeck et al., 1979). Shortly thereafter, a number of articles described the use of the TFK moiety as an inhibitor of esterases, including juvenile hormone esterase (Hammock et al., 1982, 1984), and mammalian enzymes (Ashour and Hammock, 1987). The large number of TFK-containing CE inhibitors reported in the literature has been extensively analyzed via quantitative structure-activity relationship (QSAR) techniques using juvenile hormone esterase (Székács et al., 1992; Rosell et al., 1996; Wheelock et al., 2002, 2003). In general, the potency of the aliphatic TFKs exhibits a strong positive correlation with lipophilicity; however, inhibitor potency can be increased by specific substitutions that do not strongly affect the overall lipophilicity or shape of the inhibitor. This correlation breaks down with branched chain or cyclic compounds, and increasing the degree of fluorination has also been shown to increase inhibitor efficacy (Székács et al., 1992).

Further research using TFK-containing compounds showed that substitution of the  $\beta$ -carbon with a sulfur atom (Fig. 1) led to a significant increase in inhibitor potency (Hammock et al., 1984; Ashour and Hammock, 1987). The sulfur atom was initially incorporated into TFK inhibitors to serve as a bioisostere of the olefin group in juvenile hormone. However, the resulting increase in compound efficacy was greater than expected and led to alternative hypotheses regarding the role of the sulfur atom (Székács et al., 1992). It is possible that this atom is involved in intramolecular hydrogen bonding with the ketone and/or *gem*-diol (Székács et al., 1992), thereby shifting the equilibrium toward the latter form. On the other hand, the sulfur may be involved in  $\pi$ -orbital stacking or other interactions with amino acid residues within the enzyme active site (Wheelock et al., 2002). A recent study has elucidated some of the physical interactions that the sulfur atom undergoes in juvenile hor-

mone esterase; however, the effects upon mammalian enzymes are still unclear.

In this article, we have examined the inhibition of three recombinant mammalian CEs by a series of TFKs, and we determined 3D-QSAR pseudoreceptor models that account for their biological activity. These results demonstrate not only that differences in inhibitor structure affect enzyme inhibition (e.g., the length of the alkyl chain) but also that subtle differences within the CE active sites significantly influence the potency of these compounds. These data will be of particular use in comparing differences between insect and mammalian CE structure activity relationships. In addition, these inhibitors may also prove useful for elucidating the endogenous role of these enzymes, or for affinity purification of esterases and related enzymes.

## Materials and Methods

### Enzyme and Inhibitors

hCE1 and rCE were purified as described previously (Morton and Potter, 2000). hiCE was purified in a similar manner; however, the enzyme was only approximately 50% pure. Contaminating proteins in this sample included BSA and baculoviral proteins that have been shown not to affect kinetic studies with this enzyme (Wadkins et al., 2004). The Genbank accession numbers for the cDNAs encoding the CEs used in these studies were as follows; hiCE, Y09616 (Schwer et al., 1997); hCE1, M73499 (Munger et al., 1991); and rCE, AF036930 (Potter et al., 1998).

hAChE and hBChE were obtained from Sigma Biochemicals (St. Louis, MO). The ether, sulfanyl, and sulfonyl TFK inhibitors (Table 1) were synthesized as described previously (Wheelock et al., 2001, 2002). Compound **7** (1,1,1-trifluorododecan-2-one) was synthesized according to the methods of Hammock et al. (1982). Compounds were characterized by <sup>1</sup>H NMR and mass spectrometry, and all data were in agreement with previously published values. The structures of all compounds tested are shown in Table 1. Inhibitors are shown as either the ketone or hydrate based upon the presence of a *gem*-diol signal by <sup>1</sup>H NMR (two broad down-field singlets when acquired in CDCl<sub>3</sub>). Inhibitors were dissolved in dimethyl sulfoxide immediately before use.

### Synthesis of 1,1,1-Trifluoro-3-(alkylsulfinyl)propane-2,2-diols

The 1,1,1-trifluoro-3-(alkylsulfinyl)propane-2,2-diols (alkyl TFK sulfoxides) were synthesized via the same general procedure as the above compounds. To the corresponding thioether (1 eq) in 0.1 M dichloromethane at 0°C was added *m*-chloroperoxybenzoic acid (1 eq). The reaction was stirred overnight and washed with 1 M K<sub>2</sub>CO<sub>3</sub>, and the organic layer was dried with Na<sub>2</sub>SO<sub>4</sub>. After filtering, the solvent was removed under reduced pressure; the target compound was recovered by recrystallization from dichloromethane/hexane in 30 to 35% yield. Physical parameters of the compounds are indicated below.

**1,1,1-Trifluoro-3-(butylsulfinyl)propane-2,2-diol.** <sup>1</sup>H (300 MHz, CDCl<sub>3</sub>): 6.37 (br, 1H), 5.17 (br, 1H), 4.20–4.00 (m, 0.3 H), 3.20–2.80 (m, 4H), 1.90–1.70 (m, 2H), 1.60–1.40 (m, 2H), 0.99 (t, *J* = 0.97 Hz, 3H); Mp = 79–82°C.

**1,1,1-Trifluoro-3-(hexylsulfinyl)propane-2,2-diol.** <sup>1</sup>H (300 MHz, CDCl<sub>3</sub>): 6.34 (br, 1H), 4.76 (br, 1H), 4.15–4.00 (m, 0.4 H), 3.15–2.80 (m, 4H), 1.90–1.70 (m, 2H), 1.60–1.25 (m, 6H), 0.89 (m, 3H); Mp = 89–91°C.

**1,1,1-Trifluoro-3-(octylsulfinyl)propane-2,2-diol.** <sup>1</sup>H (300 MHz, CDCl<sub>3</sub>): 6.36 (br, 1H), 4.88 (br, 1H), 4.15–4.00 (m, 0.16 H), 3.15–2.80 (m, 4H), 1.90–1.70 (m, 2H), 1.60–1.25 (m, 10H), 0.89 (m, 3H); Mp = 87–90°C.

**1,1,1-Trifluoro-3-(decylsulfinyl)propane-2,2-diol.** <sup>1</sup>H (300 MHz, CDCl<sub>3</sub>): 6.35 (br, 1H), 4.76 (br, 1H), 4.17–4.00 (m, 0.16 H),

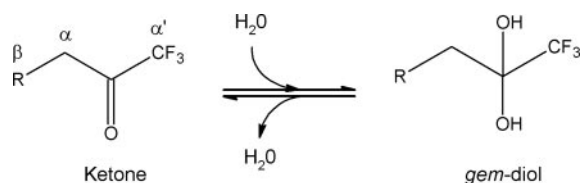


**Fig. 1.** Interconversion of the ketone and the *gem*-diol forms of the inhibitors after hydration. The naming of the atoms is indicated by the Greek letters.

TABLE 1

ID, structures, and names of the compounds assayed

Compounds are drawn in either their ketone or *gem*-diol form dependent upon the chemical structure obtained from  $^1\text{H}$  NMR spectroscopy in  $\text{CDCl}_3$ . Displayed structures were used for the QSAR molecular modeling.

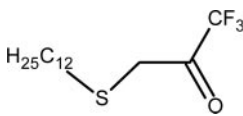
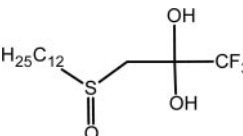
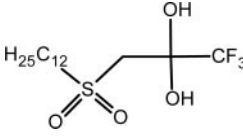
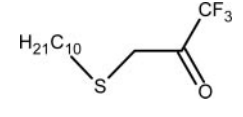
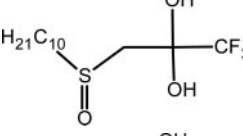
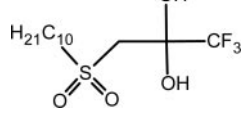
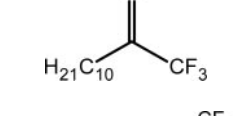
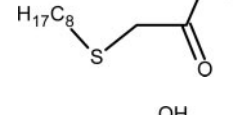
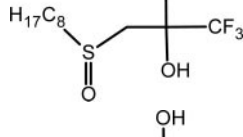
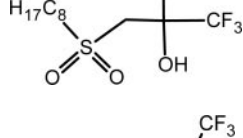
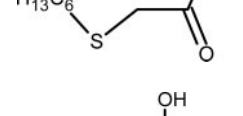
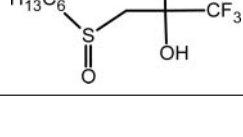
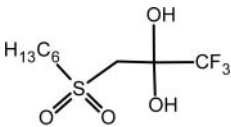
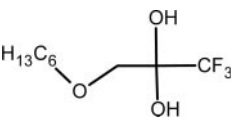
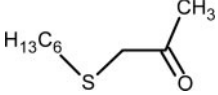
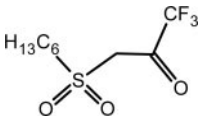
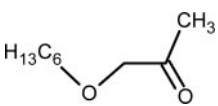
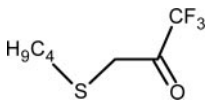
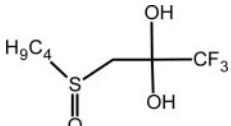
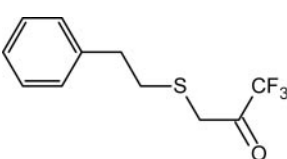
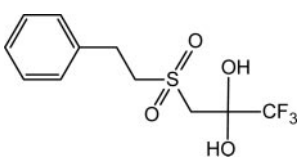
ID	Structure	Name
1		3-(Dodecylthio)-1,1,1-trifluoropropan-2-one
2		3-(Dodecylsulfinyl)-1,1,1-trifluoropropane-2,2-diol
3		3-(Dodecylsulfonyl)-1,1,1-trifluoropropane-2,2-diol
4		3-(Decylthio)-1,1,1-trifluoropropan-2-one
5		3-(Decylsulfinyl)-1,1,1-trifluoropropane-2,2-diol
6		3-(Decylsulfonyl)-1,1,1-trifluoropropane-2,2-diol
7		1,1,1-Trifluorododecan-2-one
8		1,1,1-Trifluoro-3-(octylthio)propan-2-one
9		1,1,1-Trifluoro-3-(octylsulfinyl)propane-2,2-diol
10		1,1,1-Trifluoro-3-(octylsulfonyl)propane-2,2-diol
11		1,1,1-Trifluoro-3-(hexylthio)propan-2-one
12		1,1,1-Trifluoro-3-(hexylsulfinyl)propane-2,2-diol

TABLE 1  
Continued

ID	Structure	Name
13		1,1,1-Trifluoro-3-(hexylsulfonyl)propane-2,2-diol
14		1,1,1-Trifluoro-3-(hexyloxy)propane-2,2-diol
15		1-(Hexylthio)propan-2-one
16		1-(Hexylsulfonyl)propan-2-one
17		1-(Hexyloxy)propan-2-one
18		3-(Butylthio)-1,1,1-trifluoropropan-2-one
19		3-(Butylsulfinyl)-1,1,1-trifluoropropane-2,2-diol
20		1,1,1-Trifluoro-3-(phenethylthio)propan-2-one
21		1,1,1-Trifluoro-3-phenethylsulfonyl propane-2,2-diol

3.20–2.80 (m, 4H), 1.90–1.70 (m, 2H), 1.60–1.25 (m, 14H), 0.88 (m, 3H); Mp = 90–95°C.

**1,1,1-Trifluoro-3-(dodecylsulfinyl)propane-2,2-diol.** <sup>1</sup>H (300 MHz, CDCl<sub>3</sub>): 6.32 (br, 1H), 4.70 (br, 1H), 4.20–4.00 (m, 0.05 H), 3.20–2.80 (m, 4H), 1.90–1.70 (m, 2H), 1.60–1.25 (m, 18H), 0.86 (m, 3H); Mp = 98–100°C.

#### Predicted Water Solubilities and logP Values of Inhibitors

Water solubilities and logP values were predicted using Chem-Silico Predict v2.0 software (ChemSilico LLC, Tewksbury, MA).

#### Carboxylesterase Inhibition

Inhibition of CEs was assessed using 3 mM *o*-nitrophenyl acetate (*o*-NPA) as a substrate in 50 mM HEPES, pH 7.4, over a 5-min time

period (Wadkins et al., 2004, 2005). Inhibitor was added either simultaneously with *o*-NPA or after a 24-h preincubation (in the absence of substrate). Assays were routinely performed in duplicate in multiwell plates using at least eight concentrations of inhibitor, ranging from 1 pM to 100 μM. Positive (50 μM bis-4-nitrophenyl phosphate) and negative (dimethyl sulfoxide) controls were included in all assays.

#### Acetylcholinesterase and Butyrylcholinesterase Inhibition

Inhibition of hAChE and hBChE was assessed using multiwell plate assays as described previously (Doctor et al., 1987; Morton et al., 1999; Wadkins et al., 1999, 2004, 2005).



## Analysis of Enzyme Inhibition

To determine the  $K_i$  values and the mode of enzyme inhibition, data were fitted to the following equation (Webb, 1963; see Scheme 1).

$$i = \frac{[I]\{[S](1 - \beta) + K_s(\alpha - \beta)\}}{[I]\{[S] + \alpha K_s\} + K_i\{\alpha[S] + \alpha K_s\}} \quad (1)$$

where  $i$  = fractional inhibition,  $[I]$  = inhibitor concentration,  $[S]$  = substrate concentration,  $\alpha$  = change in affinity of the substrate for the enzyme in the presence of the inhibitor,  $\beta$  = change in the rate of enzyme substrate complex decomposition in the presence of the inhibitor,  $K_s$  is the dissociation constant for the enzyme substrate complex (assuming negligible commitment to catalysis), and  $K_i$  is the inhibitor constant. The data sets were analyzed using GraphPad Prism software and Perl Data Language, and the mode of enzyme inhibition was determined by evaluating the  $r^2$  values for the curve fits using Akaike's information criteria (Wadkins et al., 2005).  $K_i$  values were then calculated using the best-fit model described from these analyses.

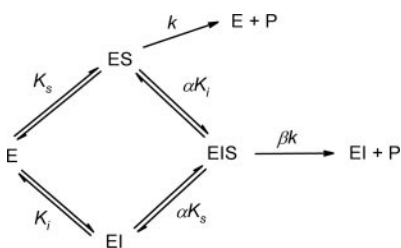
In most cases, enzyme inhibition was either partially competitive (i.e., where the inhibitor does not affect the rate of enzyme/substrate complex dissociation and only partially hinders substrate binding) or partially noncompetitive (i.e., where the binding of substrate to the enzyme is unaffected by the inhibitor, but the dissociation of the enzyme/inhibitor/substrate complex is slower than that of the enzyme/substrate complex).

Analysis of datasets obtained from preincubation of the enzyme with the inhibitor for 24 h indicated that, in some instances, the "on" rate for the small molecules was very slow (and/or that the formation of enzyme/inhibitor complex occurred slowly). Because eq. 1 cannot yield accurate  $K_i$  values from the preincubation studies, we determined apparent inhibition constants ( $K_{iapp}$ ) using this equation and also reanalyzed the datasets using the approaches described previously (Morrison and Walsh, 1988). These take into consideration the slow binding of inhibitors in the absence of substrate.

Analyses of the inhibitor concentration effect on initial velocities ( $v_0$ ) of substrate conversion typically showed the characteristic pattern of a "mechanism B" type inhibitor. This type of inhibitor has been extensively reviewed (Morrison and Walsh, 1988) and is described by the mechanism of Webb (1963), except that the EIS complex is not formed, and the inhibitor forms a new isomer species ( $EI^*$ ) that can revert to the EI complex. Under these conditions, the inhibition of initial velocities ( $v_0$ ) is given by:

$$v_0 = \frac{V_{max}[S]}{K_M \left(1 + \frac{[I]}{K_i}\right) + [S]} \quad (2)$$

where  $K_M$  is determined in the absence of inhibitor,  $[I]$  is the inhibitor concentration,  $[S]$  is the substrate concentration, and  $V_{max}$  is the maximum velocity achieved in the presence of the inhibitor. This equation holds true where the conversion from  $EI^*$  to EI is rapid, relative to the reverse reaction.



**Scheme 1.** A schematic indicating the potential reaction mechanism for the formation of product (P) for the enzyme (E)/substrate (S) equilibrium in the presence of inhibitor (I). The constants  $\alpha$ ,  $\beta$ ,  $K_s$ ,  $K_i$ , and  $k$  are described in the text.

## Molecular Modeling of Inhibitors of Carboxylesterase

3D-QSAR analyses were performed using Quasar 5.0 (Stewart, 1990; Vedani and Dobler, 2002a,b; Vedani et al., 2005) running on a Macintosh G4 computer. Structures for each analog were initially constructed with Chem3D for Macintosh (CambridgeSoft, Cambridge, MA) using the compounds shown in Table 1 (i.e., compound 1 was constructed as the ketone and compound 2 as the *gem*-diol). Partial atomic charges from the bond charge correction method (Jakalian et al., 2002) and AMBER atom types were assigned using the *antechamber* module of AMBER7 (University of California, San Francisco, CA). Structures for QSAR analysis were performed by initial energy minimization of compound 4 using the PM3 Hamiltonian of MOPAC (Stewart, 1990). All analogs were then aligned using the decyl chain and the S-C-C = O dihedral of 4 as a template.

## Results

**Inhibition of CE by TFKs and Their Structural Analogs.** To assess the ability of the TFKs to inhibit CEs, inhibition studies were performed using *o*-NPA as a substrate, and  $K_i$  values were determined for each inhibitor (Table 1) with each enzyme. As indicated in Tables 2 and 3, the thioether TFKs (compounds 1, 4, 8, 11, 18, and 20) were all potent inhibitors of the three different mammalian CEs, with  $K_i$  values ranging from 0.3 to 1670 nM. For the 5-min data sets (Table 2), the potency of enzyme inhibition was clearly related to the length of the alkyl chain. For example, the butyl derivative (18) was ~100-fold less potent against hiCE compared with the dodecyl analog (1), with the intermediate length molecules falling within this range. Plots of the data sets comparing the  $K_i$  values with the number of carbon atoms in the alkyl moiety yielded linear relationships (Fig. 2A). The  $r^2$  values for these curve fits were 0.937, 0.981, and 0.754 for hiCE, hCE1, and rCE, respectively. It is noteworthy that the change in potency afforded by the alkyl group was much more pronounced in hiCE compared with rCE, as evidenced by the differences in the slopes of the lines in Fig. 2.

However, similar analyses using the data derived from the 24 h inhibition assays (Table 3), did not yield such relationships, with  $r^2$  values ranging from 0.07 to 0.1 (data not shown). These results suggest that the initial interaction of the inhibitor and the enzyme is modulated by the alkyl chain length.

In the short-duration assays (5 min), the sulfinyl *gem*-diol TFKs (RS(O)CH<sub>2</sub>C(OH)<sub>2</sub>CF<sub>3</sub>; compounds 2, 5, 9, 12, and 19) were all weaker CE inhibitors. This trend was also dependent upon alkyl chain length. For example, with hiCE, compounds with long alkyl chains (e.g., 2), exhibited only a ~3.5-fold reduction in potency relative to the thioether analog (1). However, the shorter chain analog (12) showed a ~120-fold reduction in potency (Table 1). In addition, the butyl derivative (19) was inactive against all the enzymes examined in this assay system. In general, these sulfoxide-containing analogs were 10- to 30-fold weaker in their ability to inhibit CEs.

In contrast, in the 24 h assays, the sulfinyl *gem*-diol TFKs were more potent at CE inhibition than the thioether analogs. For example, compound 5 demonstrated  $K_i$  values of 1.9, 5.3, and 2.5  $\mu$ M for hiCE, hCE1, and rCE, respectively, when assayed over 5 min. However, this same molecule displayed  $K_{iapp}$  values of 6.6, 0.5, and 16.1 nM after incubation with the same panel of enzymes for 24 h. Hence, for this compound, it is likely that the "on" rate for the CEs is slow and that the

ably reduced, with most values ranging from 0.59 to 376 nM. The exception was compound **16**, where  $K_{iapp}$  values were considerable larger (450–18,300 nM).

As indicated earlier, it is likely that the "on/off" rate of the inhibitors would significantly affect substrate hydrolysis, especially under conditions in which the enzyme had been preincubated with the compounds for extended periods of

$K_{iapp}$  values for the inhibition of h1CE, hCE1, rCE, hAChE, or hBChE after preincubation of the enzymes with the TFK analogs for 5 min. Data were analyzed using Eq. 1 and are presented  $\pm$  S.E.

Modes of enzyme inhibition are:

- <sup>a</sup> Competitive.
- <sup>b</sup> Partially noncompetitive.
- <sup>c</sup> Partially competitive.

$K_{\text{app}}$  values for the inhibition of hCE, hCE1, rCE, hAChE, or hBChE after preincubation of the enzymes with the TFK analogs for 24 h. Data were analyzed using Eq. 1 and are presented  $\pm$  S.E.

Modes of enzyme inhibition are:

- <sup>a</sup> Partially noncompetitive.
- <sup>b</sup> Partially competitive.
- <sup>c</sup> Competitive.
- <sup>d</sup> Noncompetitive.

time. Therefore, we reanalyzed the 24 h datasets using the model described by Morrison and Walsh (1988). Using this approach, we fitted the  $v_o$  data versus inhibitor concentration using nonlinear least-squares analysis to obtain  $K_i$  for the compounds (Table 4). In general, the values were similar to the partial competitive and partial noncompetitive data given in Table 3, indicating that both the general analysis and the more specialized slow-binding analysis could be used to interpret our inhibitor data. There are a few exceptions, notably compounds **7**, **16**, and **20**. It is clear that the  $K_i$  values obtained with these analogs are significantly dependent on the model chosen to fit the data. We have therefore provided both  $K_{iapp}$  and  $K_i$  values to acknowledge this point.

It is noteworthy that some of the compounds demonstrated inhibitory activity toward both hAChE and hBChE. For example, compound **4** exhibited  $K_i$  values of  $\sim 700$  nM and  $\sim 11$   $\mu$ M with hAChE and hBChE, respectively, after 5-min incubation. It is unclear why this particular compound, which has an alkyl chain consisting of 10 carbon atoms, would be effective as an inhibitor, compared with compounds **1** ( $C_{12}$ ) and **8** ( $C_8$ ). However, in general, inhibition of the cholinesterases was weak and occurred only at much higher inhibitor concentrations (typically  $>10$   $\mu$ M).

**Correlations between the  $K_i$  Values and the ClogP or the Water Solubilities of the TFK Inhibitors.** As indicated above, the  $K_i$  values obtained from the 5-min assays were correlated with the length of the alkyl chain within the thioether TFK-containing inhibitors (Fig. 2A). Because the active sites of the mammalian CEs are lined with aromatic amino acids that create a highly hydrophobic domain within the protein, we hypothesized that the ClogP values and/or the water solubility of the compounds may also correlate with their inhibitory potency. Therefore, the ClogP values and the water solubilities of the inhibitors were predicted from their chemical structures using ChemSilico Predict software (Table 5). Graphical plots of these datasets with the  $K_i$  values for the different enzymes are depicted in Fig. 2, B and C. Good correlations between these parameters were observed, consistent with previous results seen in Fig. 2A. Because the length of the alkyl group, the hydrophobicity of the molecules, and the water solubility of the inhibitors are inversely related, it is perhaps not surprising that there is a correlation with the inhibitory potency of these compounds. However, it

is clear that these simple models may have some predictive power toward the design of novel TFK inhibitors.

As mentioned above, no correlations between these parameters were observed with the data obtained after preincubation of the inhibitor with the enzymes for 24 h. This suggests that the initial interaction of the thioether TFKs with the CEs is modulated by the alkyl group, but over extended periods of time this effect is minimized.

**Molecular Modeling of TFK-Mediated Inhibition of CEs.** To assess the contribution of the chemical properties of the molecules toward enzyme inhibition, 3D-QSAR analyses were performed using Quasar 5.0 software (Vedani and Dobler, 2002a,b; Vedani et al., 2005). Only those analogs from Table 3 that displayed partial noncompetitive inhibition were used to generate the pseudoreceptor models. The  $K_i$  values predicted for the inhibitors that operate by other mechanisms were then compared.

TABLE 4

$K_i$  values for the inhibition of hiCE, hCE1, or rCE after preincubation of the enzymes with the TFK analogs for 24 h  
 Datasets were analyzed using the model applicable for slow binding inhibitors (eq 2). Data are presented as mean  $\pm$  S.E.

ID	$K_i$		
	hiCE	hCE1	rCE
<i>nM</i>			
<b>1</b>	$5.4 \pm 1.9$	$7.4 \pm 1.5$	$3.3 \pm 1.0$
<b>2</b>	$0.4 \pm 0.1$	$0.4 \pm 0.1$	$1.4 \pm 0.2$
<b>3</b>	$1.0 \pm 0.2$	$0.4 \pm 0.1$	$0.7 \pm 0.1$
<b>4</b>	$4.6 \pm 1.2$	$4.0 \pm 0.9$	$2.8 \pm 0.4$
<b>5</b>	$0.5 \pm 0.1$	$0.5 \pm 0.1$	$3.0 \pm 0.3$
<b>6</b>	$1.1 \pm 0.3$	$0.3 \pm 0.1$	$1.6 \pm 0.2$
<b>7</b>	$2043.3 \pm 146.8$	$2.3 \pm 0.2$	$3236.6 \pm 271.1$
<b>8</b>	$3.50 \pm 0.6$	$4.2 \pm 0.9$	$7.8 \pm 0.9$
<b>9</b>	$0.5 \pm 0.1$	$0.6 \pm 0.1$	$6.4 \pm 1.1$
<b>10</b>	$5.8 \pm 1.7$	$0.6 \pm 0.1$	$36.8 \pm 7.2$
<b>11</b>	$6.5 \pm 0.9$	$5.2 \pm 1.1$	$9.9 \pm 1.3$
<b>12</b>	$0.5 \pm 0.2$	$3.3 \pm 0.3$	$21.7 \pm 3.4$
<b>13</b>	$3.7 \pm 0.7$	$0.7 \pm 0.1$	$34.3 \pm 7.6$
<b>14</b>	$1.2 \pm 0.2$	$1.0 \pm 0.2$	$1.7 \pm 0.1$
<b>15</b>	$>100,000$	$>100,000$	$>100,000$
<b>16</b>	$577.9 \pm 89.2$	$1840.8 \pm 560.3$	$2516.3 \pm 229.8$
<b>17</b>	$>100,000$	$>100,000$	$>100,000$
<b>18</b>	$16.5 \pm 1.9$	$5.4 \pm 0.7$	$7.7 \pm 1.2$
<b>19</b>	$2.0 \pm 0.6$	$14.3 \pm 4.2$	$137.3 \pm 34.2$
<b>20</b>	$4.8 \pm 0.9$	$6.4 \pm 1.8$	$5.5 \pm 0.8$
<b>21</b>	$116.2 \pm 37.4$	$6.0 \pm 1.3$	$106.4 \pm 32.0$

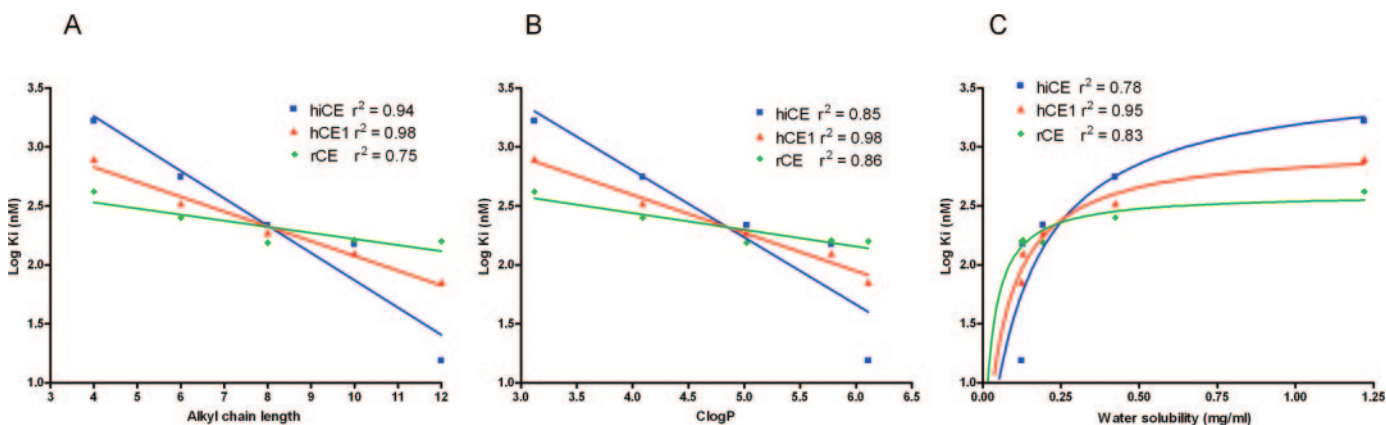


**Fig. 2.** Correlation of  $K_i$  values for CE inhibition with length of the alkyl moiety (A), the ClogP of the inhibitor (B) or the water solubility of compounds **1**, **4**, **8**, **11**, and **18**. In all graphs, data points and computer-predicted curve fits are indicated in blue for hiCE, red for hCE1, and green for rCE. Goodness of fit coefficients ( $r^2$ ) for the lines are indicated on the graphs.



The  $r^2$  correlation coefficients for the predicted versus experimental  $K_i$  values for hiCE, hCE1, and rCE are shown in Fig. 6 and Table 3. These results indicate that the models obtained from these analyses are highly correlative. To determine whether these models may have predictive power for TFKs of unknown biological activity, the cross-correlation coefficients ( $q^2$ ) were calculated. These

TABLE 5  
Predicted logP values and water solubilities for the thioether TFKs

Compound	logP	Water Solubility mg/ml
1	6.11	0.124
4	5.78	0.129
8	5.02	0.193
11	4.09	0.424
18	3.12	1.22

TABLE 6  
Correlation coefficients for the TFK CE QSAR models

Time and Enzyme	Observed versus Predicted $K_i$ ( $K_{iapp}$ ) Values ( $r^2$ )	Cross-Correlation Coefficient ( $q^2$ )	$q^2/r^2$
5 min			
hiCE	0.908	0.900	0.991
hCE1	0.943	0.896	0.950
rCE	0.948	0.900	0.949
24 h			
hiCE	0.941	0.900	0.956
hCE1	0.935	0.900	0.963
rCE	0.937	0.900	0.961

values were  $\sim 0.9$  for all enzymes under both experimental conditions (Table 6). Again, these results suggest that the models would have considerable predictive power for TFKs with unknown biological activity. An alternative measure of the significance of these analyses is demonstrated in Table 6, which displays the  $q^2/r^2$  values for the datasets. As indicated, these values are close to unity, suggesting that the models derived from these QSAR studies are highly correlative and predictive.

**3D-QSAR Pseudoreceptor Models of TFK-Mediated Inhibition of CEs.** Using the Quasar software, 3D pseudoreceptor models for the TFK analogs were generated from the inhibition data sets, and the enzyme-ligand binding sites are shown in Fig. 4. The 24-h inhibition datasets were used for model construction because these conditions were most likely to offer a more accurate representation of the equilibrium established between enzyme and inhibitor. The pseudoreceptor models generated for the TFK analogs (Fig. 4) are remarkably similar in structure to those obtained from the QSAR analysis of the previously characterized benzil- and sulfonamide-based CE inhibitors (Wadkins et al., 2004, 2005). These models accurately reflect the charged amino acid residues in the active site gorges of the CEs examined. Although it is impossible to assign a direction to the pseudoreceptor models, we anticipate that the orientation shown in Fig. 4 has the entrance to the gorge at the top and the active site, containing the catalytic residues, at the bottom. This is logical inasmuch as the bottom of the gorge contains charged

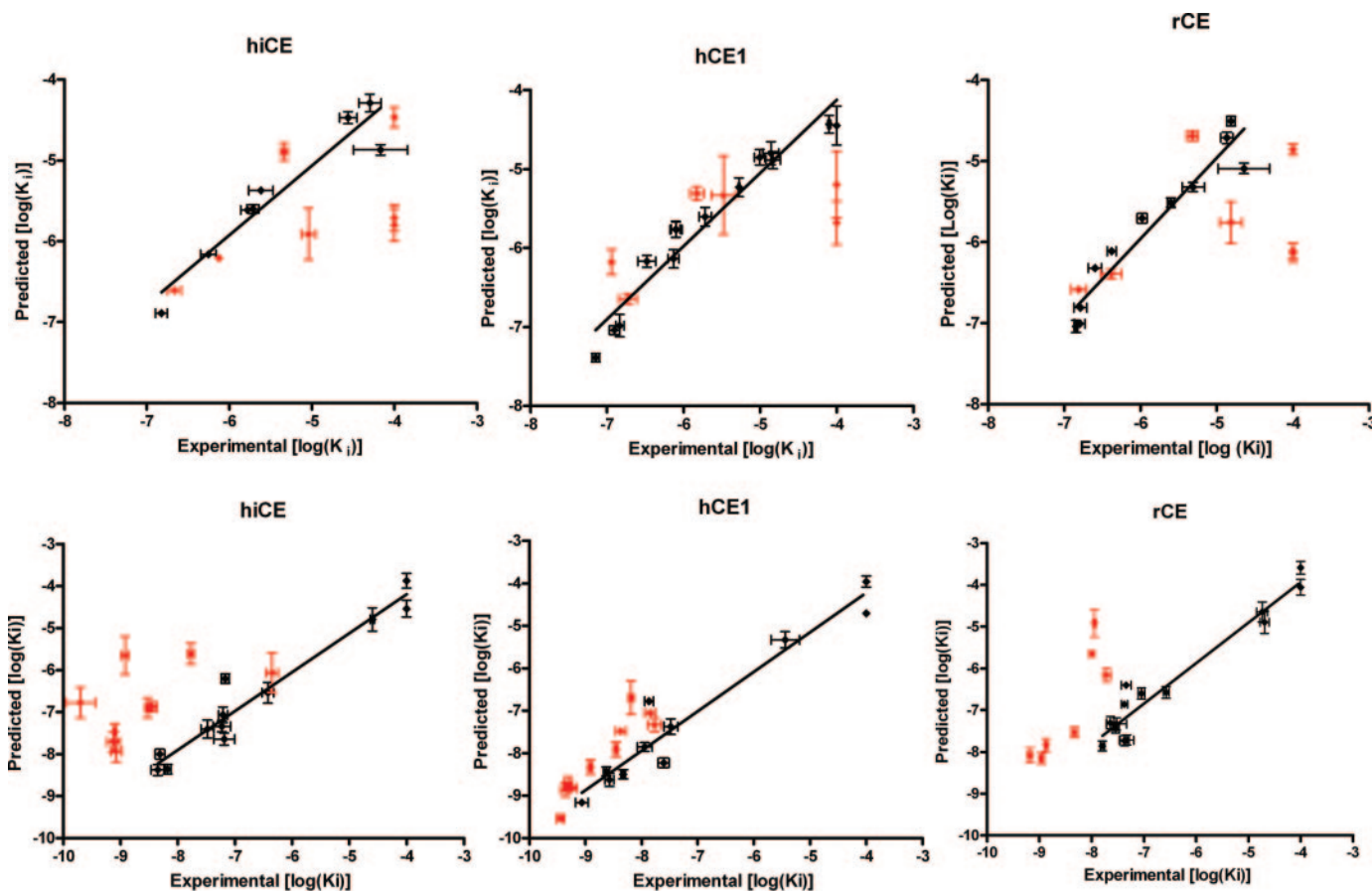


Fig. 3. Graphs of observed versus predicted  $K_i$  values for CE inhibition with the TFK analogs. Top, data points derived from the 5-min assays. Bottom, 24 h preincubation. Data depicted in black represent those used to define the QSAR models, and the validation sets are shown in red.



residues, whereas the central portion is lined with mostly hydrophobic residues.

The interpretation of the models in this manner is then straightforward with regard to the differential activities of the different inhibitors. For hCE1, less charge density is found near the bottom of the gorge than for the other CEs. Hence, compounds such as **7**, which contains a hydrophobic trifluoromethyl group and lacks an electron withdrawing carbonyl oxygen atom, inhibits hCE1 better than the other CEs. In contrast, the models more accurately predict the inhibition of hiCE and rCE by the TFK analogs, as depicted by the cationic areas present at the bottom of the active site gorge. These regions presumably facilitate hydrogen bonding of amino acids with the sulfinyl and sulfonyl oxygen atoms. However, compared with the benzil analogs (Wadkins et al., 2005), the models for the different enzymes show more similarity to each other, and the putative active site (bottom of the figure) has the most significant differences. Consequently, the enzyme selectivity that was observed with the benzil analogs was not seen with the TFK compounds. In general, the ability of the models to fit the  $K_i$  data were good (Fig. 3), indicating that they should allow for the accurate prediction of inhibitory potency and development of other TFK-containing compounds.

## Discussion

In this study, we examined the ability of TFKs to inhibit human and rabbit CEs and present detailed QSAR models describing the inhibition. The  $K_i$  values for enzyme inhibition were as low as 0.3 nM and, in general, these compounds were selective for CEs. Weaker inhibition of hAChE and hBChE was observed with the thioether-containing compounds; however, in all cases in which inhibition of the cholinesterases was seen, the influence on substrate turnover was limited. The most potent CE inhibitors (compound **1** for the 5 min assay and compound **6** for the 24 h assay) demonstrated no inhibition of hAChE or hBChE at concentrations up to 100  $\mu$ M (Tables 2 and 3). In addition, the presence of the phenyl

ring in the R group (compound **20**) significantly reduced the inhibitory potency of the molecules toward the cholinesterases compared with the CEs. This observation is consistent with our previous studies using ethane-1,2-dione-based inhibitors of esterases, which indicated that the hydrophobicity and aromaticity of the molecules significantly affected their inhibitory potency toward esterases (Hyatt et al., 2005; Wadkins et al., 2005).

The hypothesis that increased hydrophobicity correlates with inhibitor potency has been corroborated with the studies described here, which indicate that compounds containing longer, more hydrophobic alkyl chains are more potent inhibitors of CEs ( $C_{12} > C_{10} > C_8 > C_6 > C_4$ ; Table 2, and Fig. 2A). This trend is probably due to the fact that the active sites of these proteins exist as deep gorges within the enzymes that are lined with aromatic amino acids (Bencharit et al., 2002; Bencharit et al., 2003a,b). As a consequence, this gorge is relatively hydrophobic and hence provides a suitable milieu for localization of water intolerant domains. This effect is clearly reflected in the  $K_i$  data values (Table 2), the graphical plots (Fig. 2), and the QSAR pseudoreceptor models (Fig. 4). However, these correlations were observed only in short-term assays (5 min) and not after prolonged incubation of the inhibitor with the enzymes. This suggests that the alkyl group significantly impedes the binding of the thioether to the CE. Although the longer alkyl chains may increase the molecules' inhibitory potency toward the CEs, they also significantly reduce water solubility. This is exemplified by the calculated water solubilities and the logP values for these compounds (Table 5). Because these parameters are correlated (i.e., molecules containing longer chain alkyl groups are more hydrophobic and generally less water soluble) relatively good correlation coefficients were observed with the  $K_i$  values (Fig. 2 and Table 6). However, for the development of these inhibitors for practical uses, these physicochemical parameters will have to be taken into account to yield a compound that balances biological activity with bioavailability.

A comparison of the 5-min and 24-h datasets demonstrated that dramatic differences in the ability of some of these TFK

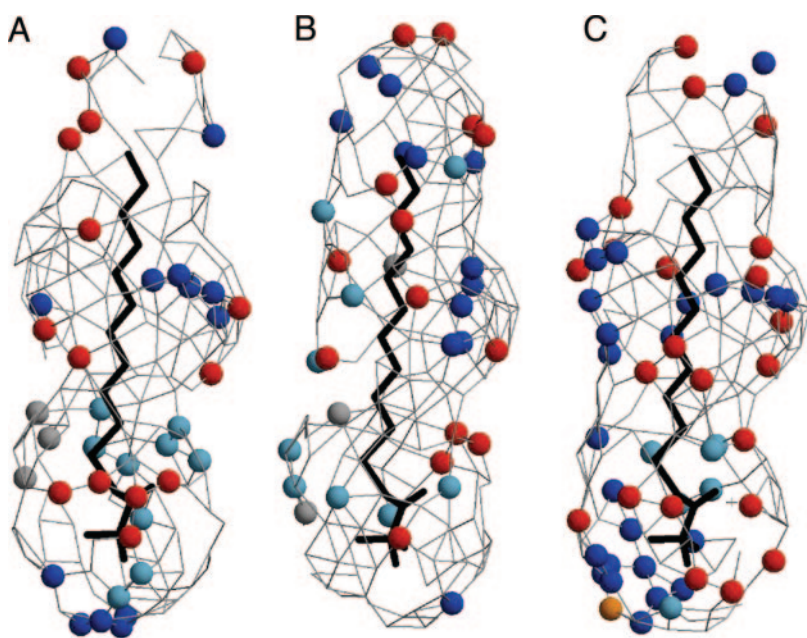


**Fig. 4.** Pseudoreceptor models that describe the best fits for the inhibition data sets derived from the 24-h preincubation assays for the TFK inhibitors. The models for hiCE (A), hCE1 (B), and rCE (C) are depicted as colored spheres on a hydrophobic gray grid. Areas that are hydrophobic are indicated in gray, whereas blue spheres represent areas that are positively charged ( $+0.1e$ ), and light blue spheres correspond to hydrogen bond donors. Orange-red spheres represent areas that are negatively charged ( $-0.1e$ ), whereas orange spheres indicate hydrogen bond acceptors. In all cases,  $e$  is the charge of the proton. The structure of compound **4** is shown in black and the figure was generated using Molscrip (Kraulis, 1991) and Raster3D (Merritt and Bacon, 1997).

analogues to inhibit the CEs. For example, compounds **12** and **13** generated  $K_i$  values ranging from 9.8 to 79.5  $\mu\text{M}$  for the different CEs in the short-term assays. However, after a 24-h preincubation with enzyme, these same inhibitors yielded  $K_{i\text{app}}$  values between 0.8 and 90 nM (0.5–34.3 nM using eq. 2). This suggests that these compounds have very slow “on” rates and that extended incubation times are required to achieve equilibrium between enzyme and inhibitor. In contrast, compound **7** produced very low  $K_i$  values for all three CEs in the 5-min assay, yet after 24-h preincubation, the  $K_{i\text{app}}$  constants had increased over 1000- and 140-fold for hiCE and rCE, respectively. We predict that for this inhibitor, the “on” rate for enzyme is very high, but the “off” rate is much slower. Hence, initially, a very high concentration of EI is formed that cannot undergo substrate binding and hydrolysis. However, after prolonged incubation, the level of EI complex would diminish (due to the loss of the inhibitor from the enzyme) and at equilibrium, substrate hydrolysis would increase, indicated by a relatively larger  $K_i$  value.

A number of studies have examined the role of the sulfur atom beta to the carbonyl carbon in inhibitor potency. It has been well established that inclusion of the sulfur atom increases inhibition of juvenile hormone esterases (Székács et al., 1992). However, the effects upon mammalian esterases have been less closely examined. A comparison of compound **8** and its analog compound **7** (in which the sulfur atom has been replaced by a methylene moiety) demonstrates an interesting result. For both human enzymes as well as rCE, the methylene analog (**7**) was a more potent inhibitor than the thioether-containing compound in the 5-min assays. However, after a 24-h preincubation, the converse is true. These results suggest that the established enzyme/inhibitor equilibrium is crucial for effective CE inhibition and indicate that the role of the sulfur atom significantly differs in mammalian and some insect esterases.

In general, the trend for inhibitor potency for a compound with a given alkyl chain length was on the order of thioether > sulfonyl > sulfinyl. The reasons for this are unclear. The data cannot be explained based upon the steric parameters of the sulfur, sulfoxide, or the sulfone moieties. One possibility is that the sulfoxide-containing compounds are highly hydrated. It has been hypothesized that the ketone is the active form of the inhibitor (Wheelock et al., 2003); however, it has also been reported that potent inhibitors exist as their hydrated forms in aqueous solution (Roe et al., 1997). If both of these reports are accurate, then the equilibrium between the ketone and *gem*-diol forms of the inhibitor must be sufficiently dynamic such that adequate concentrations of the ketone are available for enzyme inhibition. This theory is supported by the kinetic parameters of the sulfoxide-containing inhibitors, which were significantly slower than the corresponding sulfone or thioether analogs (Wheelock et al., 2002). The observation that increased enzyme/inhibitor incubation times increased the inhibition potency argues that effects upon ketone equilibrium are important for enzyme inhibition. However, it would be necessary to measure the binding constants of the individual sulfur oxidation states to fully test this hypothesis.

Analysis of the  $K_i$  values using the QSAR modeling program Quasar generated excellent observed versus predicted correlations (Fig. 3), even with relatively small data sets. Because the derived  $q^2$  values were significantly greater than

0.4, a value that is considered the cutoff for use of these models for predicting activity in biological systems (Lundstedt et al., 1998), it is likely that these models will have considerable predictive power in the design of novel TFK-based CE.

The derived pseudoreceptor models (Fig. 4) were remarkably similar in structure to those obtained after CE enzyme inhibition studies performed with a series of benzil and sulfonamide analogs (Wadkins et al., 2004, 2005; Fleming et al., 2005). These models clearly reflect the charged amino acid residues that are present within the active site gorges of hiCE, hCE1, and rCE. However, compared with the benzil pseudoreceptor models (Wadkins et al., 2005), the TFK models demonstrate greater similarity to each other for each enzyme. Consequently, the enzyme selectivity that is seen with some of the benzil analogs for the different mammalian CEs was not observed with the TFK compounds.

TFKs are slow, tight-binding inhibitors that can require significant time intervals to reach equilibrium (Wheelock et al., 2002). The kinetics of this process seems to be related to inhibitor structure, and it is therefore likely that many of the inhibitors have not reached equilibrium in short-term assays. Therefore, we compared a relatively short assay time (5 min), with a more prolonged 24-h preincubation period. Potent TFKs almost certainly exist as the *gem*-diol form in aqueous solution (Fig. 1). Therefore, the rate and/or extent of the ketone/*gem*-diol equilibrium may affect inhibitor potency. Because previous work suggested that the active form of the inhibitor is the ketone (Wheelock et al., 2003), dehydration of the *gem*-diol must occur to enable the carbonyl carbon to be subjected to nucleophilic attack by the catalytic serine. However, this process is poorly understood and will require further investigation to elucidate the mechanism of TFK-mediated CE inhibition.

Overall, these studies have elucidated parameters (e.g., alkyl chain length) that are important for the biological activity of the TFK analogs and this information, used in conjunction with the 3-D pseudoreceptor models, should be beneficial in the design of novel inhibitors. In addition, the models that were obtained from these studies were entirely consistent with those that have previously been described for the mammalian CEs (Wadkins et al., 2004, 2005). By comparison of these independent models, it is likely that subtle differences will be identified, allowing for the design of more selective and potentially more potent inhibitors. For example, a TFK-based inhibitor might combine the asymmetric trifluoropropan-2-one head group with a bulkier hydrophobic moiety. Compounds having large aromatic ring systems are excellent inhibitors of CEs (Hyatt et al., 2005; Wadkins et al., 2005); therefore, TFK analogs containing more bulky and/or aromatic moieties may become more potent inhibitors. Studies designed to assess the properties of such compounds are currently underway.

## References

- Ahmad S and Forgash AJ (1976) Nonoxidative enzymes in the metabolism of insecticides. *Ann Clin Biochem* **13**:141–164.
- Ashour MB and Hammock BD (1987) Substituted trifluoroketones as potent, selective inhibitors of mammalian carboxylesterases. *Biochem Pharmacol* **36**:1869–1879.
- Bencharit S, Morton CL, Howard-Williams EL, Danks MK, Potter PM, and Redinbo MR (2002) Structural insights into CPT-11 activation by mammalian carboxylesterases. *Nat Struct Biol* **9**:337–342.
- Bencharit S, Morton CL, Hyatt JL, Kuhn P, Danks MK, Potter PM, and Redinbo MR (2003a) Crystal structure of human carboxylesterase 1 complexed with the Alz-

- heimer's drug tacrine. From binding promiscuity to selective inhibition. *Chem Biol* **10**:341–349.
- Bencharit S, Morton CL, Xue Y, Potter PM, and Redinbo MR (2003b) Structural basis of heroin and cocaine metabolism by a promiscuous human drug-processing enzyme. *Nat Struct Biol* **10**:349–356.
- Brodbeck U, Schweikert K, Gentinetta R, and Rottenberg M (1979) Fluorinated aldehydes and ketones acting as quasi-substrate inhibitors of acetylcholinesterase. *Biochim Biophys Acta* **567**:357–369.
- Cashman J, Perroti B, Berkman C, and Lin J (1996) Pharmacokinetics and molecular detoxification. *Environ Health Perspect* **104**:23–40.
- Doctor BP, Tokar L, Roth E, and Silman I (1987) Microtiter assay for acetylcholinesterase. *Anal Biochem* **166**:399–403.
- Fleming CD, Bencharit S, Edwards CC, Hyatt JL, Tsurkan L, Bai F, Fraga C, Morton CL, Howard-Williams EL, Potter PM, et al. (2005) Structural insights into drug processing by human carboxylesterase 1: tamoxifen, mevastatin, and inhibition by benzil. *J Mol Biol* **352**:165–177.
- Hammock BD, Abdel-Aal AI, Mullin CA, Hanzlik TN, and Roe RM (1984) Substituted thiotrifluoropropanones as potent selective inhibitors of juvenile hormone esterase. *Pestic Biochem Phys* **22**:209–223.
- Hammock BD, Wing KD, McLaughlin J, Lovell VM, and Sparks TC (1982) Trifluoromethylketones as possible transition-state analog inhibitors of juvenile-hormone esterase. *Pestic Biochem Physiol* **17**:76–88.
- Hyatt JL, Stacy V, Wadkins RM, Yoon KJ, Wierdl M, Edwards CC, Zeller M, Hunter AD, Danks MK, Crundwell G, et al. (2005) Inhibition of carboxylesterases by benzil (diphenylethane-1,2-dione) and heterocyclic analogues is dependent upon the aromaticity of the ring and the flexibility of the dione moiety. *J Med Chem* **48**:5543–5550.
- Jakalian A, Jack DB, and Bayly CI (2002) Fast, efficient generation of high-quality atomic charges. AM1-BCC model: II. Parameterization and validation. *J Med Chem* **23**:1623–1641.
- Kraulis PJ (1991) MOLSCRIPT: a program to produce both detailed and schematic plots of protein structures. *J Appl Cryst* **24**:946–950.
- Linderman RJ, Upchurch L, Lonikar M, Venkatesh K, and Roe RM (1989) Inhibition of insect juvenile-hormone esterase by alpha,beta-unsaturated and alpha-acetylenic trifluoromethyl ketones. *Pestic Biochem Physiol* **35**:291–299.
- Lundstedt T, Seifert E, Abramo L, Thelin B, Nystrom A, Pettersen J, and Bergman B (1998) Experimental design and optimization. *Chemom Intell Lab Syst* **42**:3–40.
- Merritt EA and Bacon DJ (1997) Raster 3D: photorealistic molecular graphics. *Meth Enzymol* **277**:505–524.
- Morrison JF and Walsh CT (1988) The behavior and significance of slow-binding enzyme inhibitors. *Adv Enzymol Relat Areas Mol Biol* **61**:201–301.
- Morton CL and Potter PM (2000) Comparison of *Escherichia coli*, *Saccharomyces cerevisiae*, *Pichia pastoris*, *Spodoptera frugiperda*, and COS7 cells for recombinant gene expression: Application to a rabbit liver carboxylesterase. *Mol Biotechnol* **16**:193–202.
- Morton CL, Wadkins RM, Danks MK, and Potter PM (1999) CPT-11 is a potent inhibitor of acetylcholinesterase but is rapidly catalyzed to SN-38 by butyrylcholinesterase. *Cancer Res* **59**:1458–1463.
- Munger JS, Shi GP, Mark EA, Chin DT, Gerard C, and Chapman HA (1991) A serine esterase released by human alveolar macrophages is closely related to liver microsomal carboxylesterases. *J Biol Chem* **266**:18832–18838.
- Potter PM, Pawlik CA, Morton CL, Naeve CW, and Danks MK (1998) Isolation and partial characterization of a cDNA encoding a rabbit liver carboxylesterase that activates the prodrug Irinotecan (CPT-11). *Cancer Res* **52**:2646–2651.
- Redinbo MR and Potter PM (2005) Mammalian carboxylesterases: from drug targets to protein therapeutics. *Drug Discov Today* **10**:313–325.
- Roe RM, Ansbaugh DD, Venkatesh K, Linderman RJ, and Graves DM (1997) A novel geminal diol as a highly specific and stable in vivo inhibitor of insect juvenile hormone esterase. *Arch Insect Biochem Physiol* **36**:165–179.
- Rosell G, Herrero S, and Guerrero A (1996) New trifluoromethyl ketones as potent inhibitors of esterases: <sup>19</sup>F NMR spectroscopy of transition state analog complexes and structure-activity relationships. *Biochem Biophys Res Commun* **226**:287–292.
- Ross MK, Borazjani A, Edwards CC, and Potter PM (2006) Hydrolytic metabolism of pyrethroids by human and other mammalian carboxylesterases. *Biochem Pharmacol* **71**:657–669.
- Schwer H, Langmann T, Daig R, Becker A, Aslanidis C, and Schmitz G (1997) Molecular cloning and characterization of a novel putative carboxylesterase, present in human intestine and liver. *Biochem Biophys Res Commun* **233**:117–120.
- Stewart JJ (1990) MOPAC: a semiempirical molecular orbital program. *J Comput Aided Mol Des* **4**:1–105.
- Székács A, Bordás B, and Hammock BD (1992) Transition state analog enzyme inhibitors: structure-activity relationships of trifluoromethyl ketones, in *Rational Approaches to Structure, Activity, and Ecotoxicology of Agrochemicals* (Draber W and Fujita T eds) pp 219–249, CRC Press, Boca Raton, Florida.
- Vedani A and Dobler M (2002a) 5D-QSAR: the key for simulating induced fit? *J Med Chem* **45**:2139–2149.
- Vedani A and Dobler M (2002b) Multidimensional QSAR: moving from three- to five-dimensional concepts. *Quant Struct-Act Relat* **21**:382–390.
- Vedani A, Dobler M, and Lill MA (2005) Combining protein modeling and 6D-QSAR simulating the binding of structurally diverse ligands to the estrogen receptor. *J Med Chem* **48**:3700–3703.
- Wadkins RM, Hyatt JL, Wei X, Yoon KJ, Wierdl M, Edwards CC, Morton CL, Obenauer JC, Damodaran K, Beroza P, et al. (2005) Identification and characterization of novel benzil (diphenylethane-1,2-dione) analogues as inhibitors of mammalian carboxylesterases. *J Med Chem* **48**:2905–2915.
- Wadkins RM, Hyatt JL, Yoon KJ, Morton CL, Lee RE, Damodaran K, Beroza P, Danks MK, and Potter PM (2004) Identification of novel selective human intestinal carboxylesterase inhibitors for the amelioration of irinotecan-induced diarrhea: synthesis, quantitative structure-activity relationship analysis, and biological activity. *Mol Pharmacol* **65**:1336–1343.
- Wadkins RM, Potter PM, Vladu B, Marty J, Mangold G, Weitman S, Manikumar G, Wani MC, Wall ME, and Von Hoff DD (1999) Water soluble 20(S)-glycinate esters of 10,11-methylenedioxycamptothecins are highly active against human breast cancer xenografts. *Cancer Res* **59**:3424–3428.
- Webb JL (1963) *Enzyme and Metabolic Inhibitors. Volume 1. General Principles of Inhibition*. Academic Press Inc., New York.
- Wheelock CE, Colvin ME, Uemura I, Olmstead MM, Sanborn JR, Nakagawa Y, Jones AD, and Hammock BD (2002) Use of ab initio calculations to predict the biological potency of carboxylesterase inhibitors. *J Med Chem* **45**:5576–5593.
- Wheelock CE, Nakagawa Y, Akamatsu M, and Hammock BD (2003) Use of classical and 3-D QSAR to examine the hydration state of juvenile hormone esterase inhibitors. *Bioorg Med Chem* **11**:5101–5116.
- Wheelock CE, Severson TF, and Hammock BD (2001) Synthesis of new carboxylesterase inhibitors and evaluation of potency and water solubility. *Chem Res Toxicol* **14**:1563–1572.
- Wheelock CE, Shan G, and Ottea JA (2005) Overview of carboxylesterases and their role in metabolism of insecticides. *J Pestic Sci* **30**:75–83.

**Address correspondence to:** Dr. Philip M. Potter, Department of Molecular Pharmacology, St. Jude Children's Research Hospital, 332 N. Lauderdale, Memphis, TN 38105-2794. E-mail: phil.potter@stjude.org